Chemical Geology 390 (2014) 9–21

Contents lists available at ScienceDirect

Chemical Geology

journal homepage: www.elsevier.com/locate/chemgeo

High-precision Mg isotope analyses of low-Mg rocks by MC-ICP-MS

Yajun An [a], Fei Wu [a], Yuanxin Xiang [b], Xiaoyun Nan [a], Xun Yu [c], Jinhui Yang [b], Huimin Yu [a], Liewen Xie [b,*], Fang Huang [a,*]

[a] CAS Key Laboratory of Crust-Mantle Materials and Environments, School of Earth and Space Sciences, University of Science and Technology of China, Hefei 230026, Anhui, China
[b] State Key Laboratory of Lithospheric Evolution, Institute of Geology and Geophysics, Chinese Academy of Sciences, P. O. Box 9825, Beijing 100029, China
[c] State Key Laboratory for Mineral Deposits Research, School of Earth Sciences and Engineering, Nanjing University, 22 Hankou Road, Nanjing 210093, China

ARTICLE INFO

Article history:
Received 2 May 2014
Received in revised form 23 September 2014
Accepted 24 September 2014
Available online 13 October 2014

Editor: L. Reisberg

Keywords:
Mg isotopes
MC-ICP-MS
Low-Mg samples

ABSTRACT

We present a method for precise measurement of Mg isotope ratios for low-Mg rock samples (where MgO <1 wt.%) by multi-collector inductively coupled plasma-mass spectrometry (MC-ICP-MS). The efficiency of Mg purification is significantly improved by using a newly calibrated HNO_3 + HF step to remove undesired matrix elements (such as Ti, Al, Fe, and K) in low-Mg samples. We also establish that increasing the amount of Mg loaded to the chromatographic column minimized blank effects of organics leached from cation resin. All parameters that could affect the accuracy and precision of Mg isotope analyses were rigorously examined by two independent laboratories in Beijing and Hefei. The δ^{26}Mg of mono-elemental Mg standard CAM-1 measured in the two laboratories were −2.597 ± 0.042‰ (2σ, n = 49) and −2.598 ± 0.039‰ (2σ, n = 79), respectively; in house standard IGGMg1 were −1.742 ± 0.041‰ (2σ, n = 53) and −1.749 ± 0.049‰ (2σ, n = 72), respectively. The average δ^{26}Mg over ten months of two synthetic standards, made by doping IGGMg1 and IGGMg2 with matrix elements, agrees well with their recommended values, within error. The robustness of our method was further assessed by replicated analyses of sixteen rock standards with MgO contents from 0.28 wt.% to 49.4 wt.%. The δ^{26}Mg of USGS rhyolite standards RGM-1 and RGM-2 are −0.188 ± 0.031‰ (2σ, n = 35) and −0.182 ± 0.041‰ (2σ, n = 72), respectively; granite standard GA is −0.165 ± 0.038‰ (2σ, n = 57), G-2 is −0.129 ± 0.045‰ (2σ, n = 34), GS-N is −0.204 ± 0.059‰ (2σ, n = 33), GSP-2 is 0.042 ± 0.020‰ (2σ, n = 15), and GSR-1 is −0.234 ± 0.016‰ (2σ, n = 17). Based on repeated analyses of standards, the long-term external precision of our method is better than ±0.05‰ for δ^{26}Mg. This precision allows us to distinguish the fractionation of Mg isotopes in low-Mg granites and rhyolites as well as that between mantle minerals.

1. Introduction

Magnesium is one of the most abundant elements in the Earth (Millero, 1974; McDonough and Sun, 1995; Rudnick, 2003). It has three stable isotopes (^{24}Mg, ^{25}Mg, and ^{26}Mg) with relative mass difference between ^{24}Mg and ^{26}Mg of ~8%. Mg isotopes can be significantly fractionated in many cosmochemical and geochemical processes such as condensation of solar gas (Galy et al., 2000), chemical and thermal diffusion (Richter et al., 2008; Huang et al., 2009a), crustal weathering (Tipper et al., 2006; Teng et al., 2010b; Huang et al., 2012), biogeochemical processes (Black et al., 2006) and bio-mineralization (Chang et al., 2003, 2004). Mg isotope compositions are expressed as per mil deviations from that of the standard, as follows:

$\delta^{x}Mg = [(^{x}Mg/^{24}Mg)_{sample}/(^{x}Mg/^{24}Mg)_{standard} - 1] \times 1000‰$, where x refers to mass 25 or 26, and the standard is DSM-3, which has been widely used as a bracketing standard for Mg isotopes in international labs (Galy et al., 2003).

Variation of δ^{26}Mg in terrestrial materials is up to 6‰ (Young and Galy, 2004; Tipper et al., 2006; Brenot et al., 2008; Pogge von Strandmann et al., 2008; Hippler et al., 2009; Huang et al., 2009b; Young et al., 2009; Higgins and Schrag, 2010; Wombacher et al., 2011), while the range in igneous rocks is smaller than 0.7‰ because equilibrium fractionation of Mg isotopes is limited at high temperature. Many previous studies for Mg isotopes of ultramafic and mafic rocks with high MgO contents define a relatively homogenous bulk silicate Earth with δ^{26}Mg of about −0.25‰ (Teng et al., 2007, 2010a; Handler et al., 2009; Huang et al., 2009b; Yang et al., 2009; Bourdon et al., 2010; Liu et al., 2011). There are a few reports for Mg isotopes of felsic rocks with low MgO contents (e.g., rhyolites and granites) showing substantial isotope fractionations (Bolou-Bi et al., 2009; Huang et al., 2009b; Li et al., 2010). A low δ^{26}Mg signature of granite relative to the mantle value may suggest carbonate inclusion into the source of granite (Bolou-Bi et al., 2009), while a high δ^{26}Mg implies recycling of weathered silicate sediments during granite formation (Shen et al., 2009). Because of this small variability of δ^{26}Mg in igneous samples, high-precision Mg isotope data are required in order to trace the contributions of sediments to the source of granites or rhyolites (Shen et al., 2009).

* Corresponding authors.
E-mail addresses: xieliewen@mail.iggcas.ac.cn (L. Xie), fhuang@ustc.edu.cn (F. Huang).

http://dx.doi.org/10.1016/j.chemgeo.2014.09.014
0009-2541/

A growing number of studies have described Mg isotope analytical procedures for organic samples, silicate or carbonate rocks, and meteorites (Galy et al., 2002; Chang et al., 2003; Black et al., 2006; Buhl et al., 2007; Teng et al., 2007, 2010a; Tipper et al., 2008b; Bolou-Bi et al., 2009; Handler et al., 2009; Hippler et al., 2009; Huang et al., 2009b; Young et al., 2009; Higgins and Schrag, 2010; Wang et al., 2011). After the pioneering work of Lee and Papanastassiou (1974) using cation exchange resin (AG50W-X8, 200–400 mesh) to extract Mg from meteorites with 1N HNO_3 (Lee and Papanastassiou, 1974), many studies used different resins, acids or column lengths to quantitatively purify Mg from matrix elements (K, Fe, Al, Na, Ca, etc.) (Wilde et al., 2001; Galy et al., 2002; Chang et al., 2003; Bizzarro et al., 2004; Baker et al., 2005; Tipper et al., 2006; Teng et al., 2007, 2010a; Pogge von Strandmann, 2008; Bolou-Bi et al., 2009; Handler et al., 2009; Huang et al., 2009b; Shen et al., 2009; Black et al., 2010; Bourdon et al., 2010; Foster et al., 2010; Schiller et al., 2010; Wang et al., 2011; Choi et al., 2012; Bouvier et al., 2013). For example, Chang et al. (2003) presented two separate steps of ion-exchange chromatography to purify Mg in low-Mg biogenic carbonate materials (~0.1–1 wt.% $MgCO_3$) with a high (>99.9%) Mg yield. Tipper et al. (2008b) applied a standard addition method to test the accuracy of δ^{26}Mg for a few standards including olivine, basalt, and granodiorite. Bolou-Bi et al. (2009) combined AG-MP1 anion- and AG50W-X12 cation-exchange resins to purify Mg in alkali-rich samples. Huang et al. (2009b) reported δ^{26}Mg data for a number of rock and mineral standards with much larger errors in low-Mg granites than in peridotites and basalts. Li et al. (2010) performed a four-column procedure to extract Mg from low-Mg A-type granites. Teng and Yang (2014) thoroughly reviewed possible effects causing analytical artifacts for Mg isotopes.

There is still a lack of methods specifically developed for low-Mg rock samples and high-precision δ^{26}Mg data for low-Mg rock standards are still rare. There are still remarkable inconsistencies in values reported by a few laboratories for some granite standards. For instance, δ^{26}Mg for the French granite standard GA (MgO = 0.95 wt.%) ranges from -0.75 ± 0.14‰ (Bolou-Bi et al., 2009) to -0.26 ± 0.07‰ (Li et al., 2010). This discrepancy may reflect isotope heterogeneity of GA, analytical artifacts caused by matrix effects, or bracketing standard problems (Galy et al., 2001; Huang et al., 2009b; Wombacher et al., 2009; Young et al., 2009; Wang et al., 2011; Teng and Yang, 2014). Indeed, because of the higher matrix/Mg ratios, purification of low-Mg samples (such as granites and rhyolites) is more difficult than for high-Mg samples (such as peridotites and basalts). Efforts towards better purification and smaller analytical uncertainty for low-Mg samples are clearly needed.

In this study, we developed an analytical method to effectively separate Mg from large amounts of matrix elements in low-Mg rock samples. We also rigorously evaluated all potential effects on Mg isotopes during MC-ICP-MS analyses, including known issues such as the effects of matrix contamination, acid molarities, and mismatch in sample and standard Mg concentration during MC-ICP-MS analysis. Using this new method, we established δ^{26}Mg values for sixteen rock standards with MgO contents ranging from 0.28 wt.% to 49.4 wt.% (e.g., peridotites: 44.43 wt.%–49.4 wt.%; basalts: 2.16 wt.%–9.7 wt.%; andesite: 1.79 wt.%; granites: 0.42 wt.%–2.3 wt.%; and rhyolites: 0.28 wt.%). Based on replicated analyses of synthetic standards such as IGGMg1-A, IGGMg2-A, and so on, long-term external reproducibility for δ^{26}Mg is better than ± 0.05‰ (2σ), allowing us to identify sub-per mil Mg isotope fractionation in low-Mg igneous rocks and between mantle minerals.

2. Analytical method

2.1. Reference materials studied

We mainly focus on low-Mg rock standards including two USGS rhyolite standards (RGM-1, RGM-2), two French granite standards (GA, GS-N), two USGS granite standards (G-2, GSP-2), and one granite standard (GSR-1 from the National Research Center for Certified Reference Materials of China). Both rhyolite standards RGM-1 and RGM-2 were collected from Glass Mountain, California, a single block of massive obsidian near the terminal front of a Holocene obsidian flow related to Long Valley Caldera magmatic activity (United States Geological Survey, Certificate of Analysis). This homogenized, powdered rock standard RGM-1 is no longer commercially available, and thus we also measured Mg isotopes of its replacement standard, RGM-2 to assess whether any isotopic offset between standards is present. French granite standard GA is from Andlau, Bas-Rhin (France), distributed by the Centre de Recherches Pétrographiques et Géochimiques (CRPG). GS-N is from Senones, Vosges (France), distributed by the Association Nationale de la Recherche Technique (ANRT). G-2 was collected from the Sullivan quarry near Bradford, Rhode Island by Felix Chayes, Geophysical Laboratory, Carnegie Institution. GSP-2 was collected by the U.S. Geological Survey, from the Silver Plume Quarry.

2.2. Chemical purification procedure

MgO contents of these standards in this study range from 0.28 wt.% (RGM-1) to 0.96 wt.% (GSP-2), except for the granite GS-N that contains 2.3 wt.%. 5–20 mg of sample powders were weighed and fully digested to obtain ~20 μg Mg for chemical purification. All chemical procedures were carried out in a class 1000 clean laboratory equipped with class 100 laminar flow exhaust hood. A mixture of concentrated HF–HNO_3 (~3:1, v/v) (ultra-pure acids or acids made ultra-pure through double sub-boiling distillation) was used for digestion. After the initial digestion and evaporation to dryness, samples were treated with aqua regia and dried again. Samples were then refluxed with concentrated HNO_3 to remove residual fluorides and finally dissolved in 1 ml 2N HNO_3 in preparation for chromatographic column chemistry. Because of the large matrix element contents relative to Mg in low-MgO samples, we find that it is difficult to dissolve the bulk samples into 2N HNO_3 with a volume smaller than 1 ml.

Mg purification was performed in Savillex microcolumns (6.4 mm ID × 6.2 cm bed height, 30 ml reservoir) loaded with 2 ml of Bio-Rad AG50W-X12 (200–400 mesh) cation resin. Prior to any use, the resin was cleaned by rinsing with 8N HNO_3 and H_2O alternatively at least three times and it was finally stored in Milli-Q ultrapure H_2O (18.2 MΩ). Before the start of every chemical separation procedure, the resin was gently backwashed by a syringe with Milli-Q H_2O to remove air bubbles and reduce resin compaction, pre-cleaned with 4 ml 4N HNO_3 + 0.5N HF and Milli-Q H_2O alternatively three times, and then conditioned with 3 ml 2N HNO_3 twice. All columns used for Mg purification were routinely calibrated using a synthetic standard IGGMg1-A (Table 3) and well-characterized rock geo-standards like BCR-2, RGM-1, W-2, and GSR-1 (Fig. 1). Eluates were continuously collected every 1 ml. Then we added 10 ppm ^{103}Rb to all of the eluates as internal reference before measurement using an Agilent 7500a ICP-MS at the Institute of Geology and Geophysics, Chinese Academy of Science, Beijing. A series of multi-element standards were used to construct elemental calibration curves. Machine drift was corrected by interpolation from repeated analyses of the multi-element standards during a sample run. The main contribution of molecular interferences (such as $^{38}Ar^{1}H^{+}$

Table 1
Mg purification scheme.

Eluent	Vol.(ml)	Comments
2N HNO_3	3 (×2)	Conditioning
Load sample in 2N HNO_3	1	
2N HNO_3 + 0.5N HF	5	Elute Al, Ti, Fe, Li, Na
1N HNO_3	5	Elute K, Rb
	1[a]	Pre-cut collection
	22	Collect Mg
	1[a]	After-cut collection

[a] Eluent was used to test whether there is a loss of Mg or not.

Table 2
Instrumental operating parameters for Mg isotope measurements.

Instrument parameters	Neptune (IGGCAS)	Neptune plus (USTC)
RF power	1200 W	1200 W
Cooling Ar	~16 l min^{-1}	~16 l min^{-1}
Auxiliary Ar	~0.8 l min^{-1}	~0.8 l min^{-1}
Nebulizer Ar	~1.0 l min^{-1}	~1.0 l min^{-1}
Extraction voltage	−2000 V	−2000 V
Vacuum	4–8 × 10^{-9} Pa	4–8 × 10^{-9} Pa
Typical ^{24}Mg sensitivity	5–6 V ppm^{-1} (MR)	~30 V ppm^{-1} (LR)
Background of ^{24}Mg	<1 mV	<5 mV
Cones	Ni (H), sampler cone	Ni (H), Jet sampler cone
Ion lens setting	Optimized for max. intensity	Optimized for max. intensity
Sample uptake	~50 μl min^{-1}	~50 μl min^{-1}

MR: medium-resolution; LR: low-resolution.

(0.0006%) to $^{39}K^{+}$) in samples can be corrected by the subtraction of intensities in the blank solution.

2.2.1. Effect of acid molarities on Mg elution

We chose dilute nitric acids (1N or 2N) to separate Mg from other elements and test the purification efficiency of different acids (Fig. 2). Our first test used only 1N HNO_3 to purify Mg, and an excellent separation was achieved (Fig. 2a). However, this procedure consumed a large volume of 1N HNO_3 (up to 42 ml), lengthening the whole chemical purification procedure to over 30 h and requiring a large amount of reagent. Our second test, using 2N HNO_3, predictably reduced the procedure duration and volume of reagent (Fig. 2b). However, this test also indicates that solely using 2N HNO_3 it cannot separate Mg from Rb, K, Ti, and Mn, due to overlaps in elution in these elements.

In order to achieve optimal separation and minimize the duration and the amount of nitric acid used, we tested the use of a combination of 1N HNO_3 and 2N HNO_3 in the chemical purification. In the first stage of this procedure, we used 2N HNO_3 to elute most matrix cations and later switched to 1N HNO_3 to separate Rb, K, Ti, and Mn from Mg. Although such an approach can remove most matrix elements from Mg (Fig. 2c), there are still trace amounts of K and Ti that intrude into the established Mg cut. In the case of K- and Ti-rich samples, the K/Mg or Ti/Mg ratios may be high enough to produce a measureable matrix effect on Mg isotopes during MC-ICP-MS analyses. To remediate this issue, we used 2N HNO_3 + 0.5N HF instead of pure 2N HNO_3 in the first stage to shift Ti, Al, Zr, and Y peaks far from the Mg cut (Fritz et al., 1961; Handler et al., 2009; Wombacher et al., 2009). Also, the addition of HF to the eluent leads to earlier K and Fe elution, significantly reducing the tailing of K into the Mg cut, which significantly improves the purification efficiency relative to the procedure of only using nitric acid (Fig. 2d).

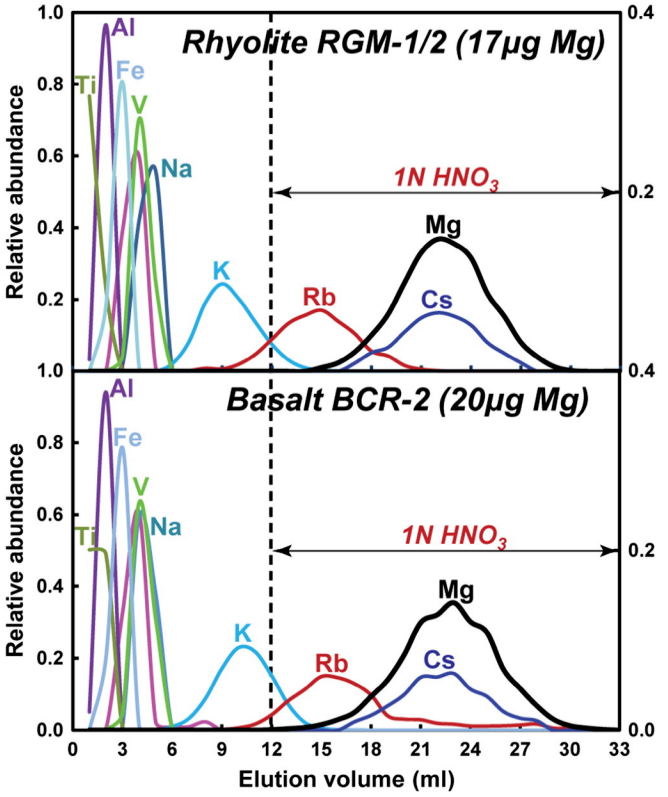

Fig. 1. Elution curves for Mg purification procedures with different rock standards. Despite containing a different set of matrix elements, the Mg peaks of the BCR-2 and RGM-1 are identical in size and location. Both the relative abundance shift of Mg lines refers to the sub-axes on the right (0–0.4), while other elements refer to the primary axes on the left (0–1). The scale on the right is expanded to show the Mg peaks more clearly.

2.2.2. Effect of Mg mass loaded on the column

Because Mg isotopes can be dramatically fractionated during ion-exchange chromatography (Chang et al., 2003; Teng et al., 2007), the Mg yield through the purification procedure is required to be close to 100%. The Mg yield is a function of the collected elution interval, where a designed column chemistry procedure captures purified Mg-bearing solutions. While a larger volume of eluent captured will often result in excellent yields, it also often introduces the tailing of matrix elements into the Mg solution. A narrow Mg cut, conversely, may result in losing Mg through incomplete capture of its elution tails. Furthermore, the expected Mg elution curve for any given column procedure will shift relative to published values, dependent on the mass of sample introduced and differing suites of matrix elements, causing further difficulty to achieve the necessary 100% recovery. Therefore, it is necessary to test the elution procedures most appropriate for different types of samples.

We generated elution curves for a variety of rock standards (DNC-1, W-2, BCR-2, GSR-1, RGM-1, and RGM-2) and the synthetic standard (IGGMg1-A) (Fig. 3). With equivalent Mg masses (~20 μg) loaded onto the resin, we find that all standards that have been processed using our column procedure have identical elution peaks, indicating that different matrices will not result in elution curve drifting. We also

Table 3
Mg isotope compositions of CAM-1, SRM980, IGGMg1, IGGMg2, and synthetic standards.

Standard[a]	$\delta^{26}Mg$	2SD	$\delta^{25}Mg$	2SD	$\delta^{26}Mg/\delta^{25}Mg$	n
Mono-elemental standards						
CAM-1_IGGCAS	−2.597	0.042	−1.343	0.036	1.935	49
CAM-1_USTC	−2.599	0.041	−1.343	0.034	1.935	70
Total average	−2.598	0.040	−1.343	0.038	1.935	119
SRM980_IGGCAS	−2.840	0.043	−1.463	0.033	1.941	70
SRM980_USTC	−2.824	0.053	−1.456	0.035	1.939	51
Total average	−2.830	0.054	−1.459	0.035	1.940	121
IGGMg1_IGGCAS	−1.742	0.041	−0.899	0.030	1.936	53
IGGMg1_USTC	−1.749	0.049	−0.907	0.034	1.928	72
Total average	−1.746	0.047	−0.904	0.033	1.932	125
IGGMg2_IGGCAS	−1.840	0.044	−0.930	0.053	1.980	9
Synthetic standards:						
IGGMg1-A	−1.766	0.042	−0.918	0.030	1.923	53
IGGMg1-B	−1.735	0.010	−0.896	0.007	1.938	8
IGGMg2-A	−1.850	0.028	−0.954	0.017	1.940	27
IGGMg2-B	−1.873	0.036	−0.967	0.017	1.937	9
IGGMg2-C	−1.865	0.051	−0.938	0.039	1.987	17
Total average	−1.858	0.039	−0.952	0.030	1.952	53

n is the number of repeat analysis of the same solution.

[a] Synthetic standards including IGGMg1-A (K: Al: Fe: Na: Ca: Mg: Mn: Rb: Ti: Zn: Cs: Cu = 20: 10: 8: 5: 5: 1: 1: 0.2: 0.1: 0.02: 0.01: 0.01); IGGMg1-B (pure Mg standard processed through the column), IGGMg2-A (K: Al: Fe: Na: Ca: Mg: Mn: Rb: Ti: Zn: Cs: Cu = 20: 40: 8: 20: 5: 1: 0.2: 0.1: 1.5: 0.02: 0.01: 0.01), IGGMg2-B (K: Al: Fe: Na: Ca: Mg: Mn: Rb: Ti: Zn: Cs: Cu = 23: 12: 3: 6: 2: 1: 0.05: 0.025: 0.4: 0.005: 0.004: 0.003), and IGGMg2-C (K: Al: Fe: Na: Ca: Mg: Mn: Rb: Ti: Zn: Cs: Cu = 12: 20: 4: 10: 3: 1: 0.1: 0.04: 0.6: 0.01: 0.01: 0.005).

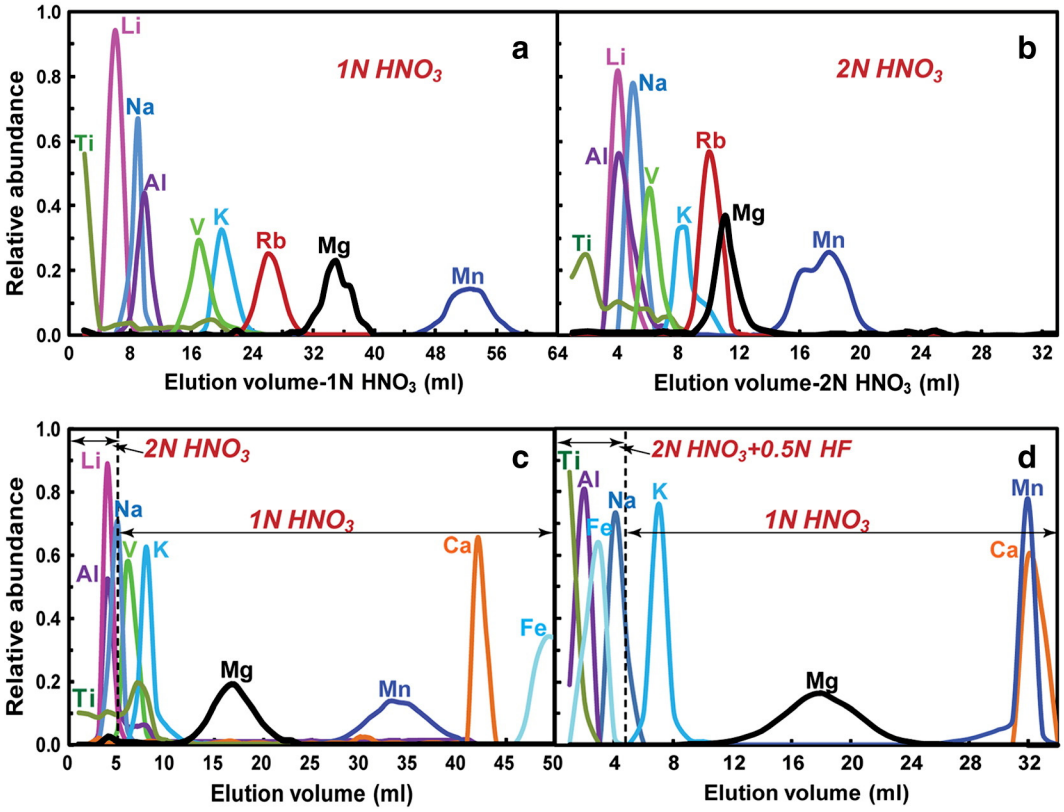

Fig. 2. Elution curves for Mg purification procedures using different reagents.

loaded different masses of Mg onto the resin, showing that the Mg peak drifts to an earlier elution and broadens with a larger mass of Mg loaded (Fig. 3). Fig. 3 only shows the interaction of the K and Mg elution peaks, as most matrix elements, including Na, were removed in 5 ml of 2N HNO_3 + 0.5N HF (Table 1). Rb does show substantial tailing on the Mg peak, but as Rb is a trace element in most samples this can be reduced to insignificant levels by passage through the column twice.

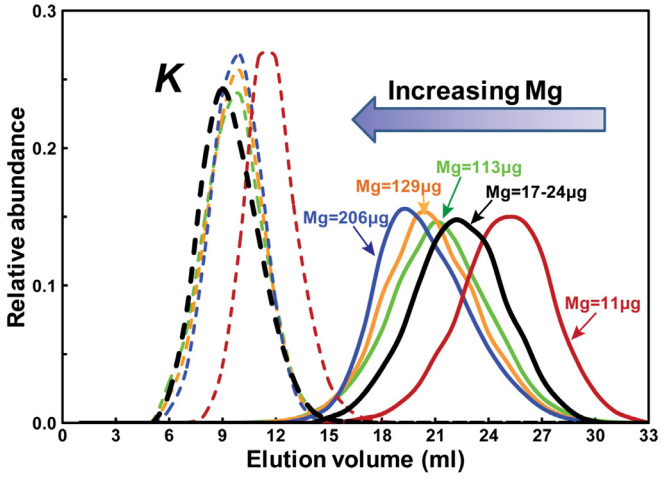

Fig. 3. Drifting of the center of the Mg and K elution curves with different masses of Mg loaded to the columns and different sample matrixes. The solid lines represent the elution of Mg, and the dashed lines represent the elution of K. Other matrix elements (such as Na, Al, Ti, and Rb) are not shown in the plot as most of them were removed in 5 ml of 2N HNO_3 + 0.5N HF or they are too low to produce significant effects on the Mg peaks. The colors correlate with different samples. Red: synthetic solution; black: rhyolite RGM-1/-2; green: basalt BCR-2; orange: dolerite W-2; and blue: diabase DNC-1. (For interpretation of the references to color in this figure legend, the reader is referred to the web version of this article.)

Taking into account this drift in the Mg peak, we collected solutions from 12 to 33 ml 1N HNO_3 as representing the Mg cut to get nearly 100% yield and excellent purification in a wide range of conditions. One milliliter aliquots before and after the 22 ml 'Mg-cut' were collected to test whether drifting of elution curves occurs. Notably, there is still a trace amount of K overlapping with the Mg cut. This is not a problem for high-Mg samples, but it may cause a significant matrix effect for samples with high K/Mg, like rhyolites. To ensure a clean separation in high-K and/or low-Mg samples, we repeated the entire purification procedure twice to greatly reduce the amount of K present.

In summary, following the chemical purification procedure outlined in Table 1, Mg can be well purified by only two column procedures from samples with large matrix/Mg ratios. Al, Na, K, Ti, and Fe can be removed earlier and Ca later than the Mg cut (Figs. 1 and 2). The Mg yields after column chemistry of pure Mg standard (IGGMg1-B), synthetic standard (IGGMg1-A), and rock reference materials are all ≥99.8%. Notably, the whole purification procedure can be conveniently finished in two days.

2.3. Mass spectrometry

Before samples were analyzed by MC-ICP-MS, the solutions were checked by ICP-MS to make sure that the purification removed most matrix elements to a level where the matrix effect is not significant (e.g., matrix/Mg ≤0.05) (Galy et al., 2001). The total procedural Mg blank was systematically lower than 6 ng, negligible relative to the amount of Mg (20 μg) processed through the column procedure.

Mg isotopes in this study were measured using a sample-standard bracketing method on a Thermo Scientific Neptune MC-ICP-MS at the Institute of Geology and Geophysics, Chinese Academy of Science (IGGCAS), Beijing. In order to test the robustness of the purification method and the analytical accuracy, some replicated samples were also measured at the University of Science and Technology of China (USTC in Hefei, Anhui Province) using a Thermo Scientific Neptune Plus MC-ICP-MS.

A "wet" plasma, using a quartz dual cyclonic-spray chamber and an ESI 50 μL min^{-1} PFA MicroFlow Teflon nebulizer (Elemental Scientific Inc., U.S.A.), was utilized to measure Mg isotopes in the mass spectrometers in the IGGCAS and USTC. A multi-collector Faraday cup configuration of L3, C, and H3 was used to measure ^{24}Mg, ^{25}Mg, and ^{26}Mg, respectively. A block of analysis consisted of 60 cycles of data with an integration time of 2.097 s per cycle. A single analysis of Mg isotope ratio is corresponded to 1 bracket using SSB method, while an analytical session consisted of ≥4 repeated runs of the same solution. An on-peak baseline was measured with 30 cycles and 1 s integration time per cycle. Cross-contamination between samples was eliminated by washing the sample-introduction system three times with 5% and 2% HNO_3 for 4 min or longer between each measurement until the ^{24} Mg signal is less than 1 mV. Instrument operating conditions are described in Table 2.

For the analyses using the Neptune in the IGGCAS, sample and standard solutions were diluted to ~2 ppm Mg in 2% (m/m) HNO_3. The signal intensity for ^{24}Mg was typically about 5–6 V/ppm. Data were collected on the flat, off-center shoulder of the mass spectrum at a medium resolution mode (M/△M ~6000). In the USTC, we used low resolution mode to analyze Mg isotopes in the Neptune Plus equipped with jet cones in order to get high sensitivity of Mg samples. No isobaric interferences were observed in Faraday cups in both instruments. The running solutions (0.5 ppm Mg in 2% HNO_3) normally produced a ^{24}Mg signal of ~15 V using the Jet cone under the low resolution. Uncertainties for $\delta^{26}Mg$ and $\delta^{25}Mg$ of standards and samples are given as two standard deviations (2σ) based on repeated measurements for at least four times.

In order to assess the quality of the mass spectrometric analyses, two international Mg standards (CAM-1 and DSM-3) (Galy et al., 2003) and two in-house reference materials (SRM980 and IGGMg1) were analyzed in both laboratories for a period over ten months. DSM-3 and CAM-1 have been well characterized in multiple laboratories (Chang et al., 2003; Galy et al., 2003; Black et al., 2006; Pearson et al., 2006; Tipper et al., 2006; Buhl et al., 2007; Pogge von Strandmann et al., 2008; Bolou-Bi et al., 2009; Hippler et al., 2009; Huang et al., 2009b; Yang et al., 2009; Young et al., 2009; Teng et al., 2010a; Choi et al., 2012; Opfergelt et al., 2012; Wimpenny et al., 2014a). SRM980 is a high-purity Mg metal obtained from the National Institute of Standards and Technology (Gaithersburg, USA). We dissolved the metal and split the solution into two bottles to make sure that the standards measured in the IGGCAS and USTC have the same Mg isotope composition. Both IGGMg1 and IGGMg2 are mono-elemental ICP-MS Mg standards (1000 ppm in 1N HNO_3) made by the National Center of Analysis and Testing for Nonferrous Metals and Electronic Materials. Results for these standard solutions are listed in Table 3. Data obtained in these two laboratories are in good agreement, within error.

3. Results and discussion

3.1. Effects of acid molarities and concentration mismatch

Purified Mg samples are normally introduced into the MC-ICP-MS in dilute nitric acid, yet previous studies have shown that different molarities of the diluting acid used in the sample-standard bracketing method may cause artifacts in metal stable isotope analyses (Malinovsky et al., 2003; Liu et al., 2014; Teng and Yang, 2014). To test and remediate the influence of diluting acid molarities on Mg isotope analyses, we bracketed 0.5 ppm IGGMg1 solutions diluted with 1 wt.% to 4 wt.% HNO_3 by 0.5 ppm IGGMg1 solution diluted by 2 wt.% HNO_3. The results from the IGGCAS and USTC laboratories indicate that the differences of acid concentration between the standards and samples will clearly produce significant isotope offsets (Fig. 4). For example, a 25% difference of acid concentration shifted the measured $\delta^{26}Mg$ value more than 0.15‰ from its accepted value. Therefore, it is critical to match the acidity of the samples and bracketing standard to avoid the mass bias difference caused by acidity mismatch. The same batch of nitric acid should be used to dilute all samples and bracketing standards, and one should also monitor for

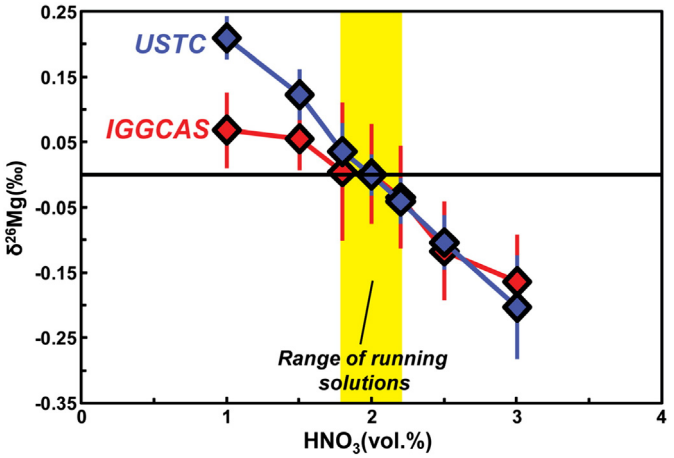

Fig. 4. $\delta^{26}Mg$ variations during measurement of Mg standard solutions diluted by different HNO_3 acid strengths. The error bars (2σ) are on the basis of at least four replicate measurements. IGGCAS: measurements in the Institute of Geology and Geophysics, Chinese Academy of Science, Beijing; USTC: measurements in the University of Science and Technology of China, Hefei, Anhui. The meanings of symbol names (IGGCAS and USTC) are same below. Errors given reflect 2σ. We measured 0.5 ppm IGGMg1 standard in variable normalities of HNO_3, bracketed by the same standard in 2% HNO_3 in the USTC. Similar behavior with 2 ppm IGGMg1 standard has been conducted in the IGGCAS. The term "range of running solutions" means the acceptable range of acid concentrations within the analytical uncertainty.

and eliminate any differences in acid molarities of the running solutions due to evaporation during the analyses (Teng and Yang, 2014).

When using a sample-standard bracketing method, the mass bias factor during analyses is also sensitive to the concentration of running solutions. To better constrain the influence of Mg concentration mismatch between samples and standards, we bracketed a series of diluted IGGMg1 solutions with a range of Mg concentrations. The recommended $\delta^{26}Mg$ value of diluted IGGMg1 relative to the concentrated solution consistently should be zero. However, we observed that increasing Mg concentration relative to the bracketing solution increases the $\delta^{26}Mg$ value. The concentration mismatch between samples and standards affects the accuracy of Mg isotope analysis to variable degrees for different types of MC-ICPMS instruments with distinct settings. Huang et al. (2009b) also found a positive correlation between the $\delta^{26}Mg$ value of the sample and the concentration ratio using 'dry' plasma on a Nu plasma MC-ICP-MS. A heavier ratio for higher concentration suggests a preferential transmission of ^{26} Mg relative to ^{24} Mg. As shown in Fig. 5, when the

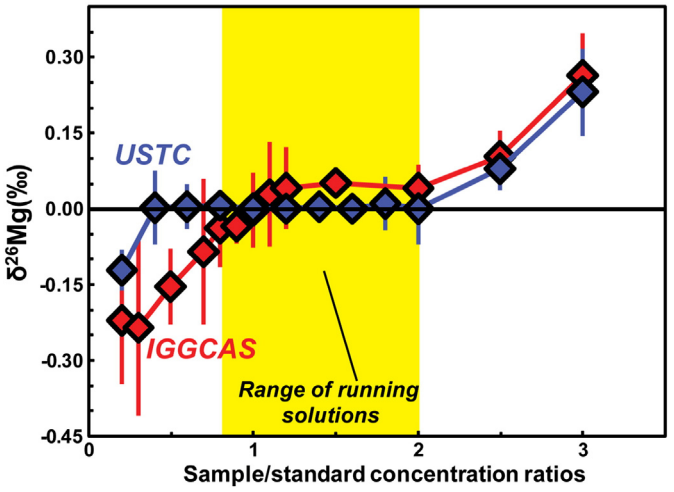

Fig. 5. Comparison of the effect of Mg concentration mismatches between sample and standard on $\delta^{26}Mg$ analyses. The Mg concentrations of the bracketing standards are 2 ppm and 0.5 ppm in IGGCAS and USTC, respectively.

difference of sample/standard Mg signal intensities is higher than 20% for the Neptune (IGGCAS), the concentration mismatch can cause a mass bias greater than 0.1‰, while the mismatch effect is insignificant in the Neptune Plus (USTC) if the sample-standard intensity ratio ranges from 0.5 to 2. Our results suggest that isotope analyses at the medium-resolution mode for the Neptune (IGGCAS) are more sensitive to the concentration mismatch than that conducted at the low-resolution mode for the Neptune plus (USTC). Such difference could be related to the instrumental mass-bias change due to the different ion beam sizes passing through the interface region and entrance slits. Nevertheless, concentrations of all samples introduced into the MC-ICP-MS in this study were carefully adjusted to within 5% difference relative to the DSM-3 solution.

3.2. Matrix effect

Matrix effects can cause significant spectrum and non-spectrum interferences on Mg isotope analyses. The most important isobaric interferences include $^{48}Ti^{++}$, $^{48}Ca^{++}$, $^{12}C^{12}C^{+}$ for ^{24}Mg, $^{50}Ti^{++}$, $^{50}Cr^{++}$, $^{12}C^{13}C^{+}$ for ^{25}Mg, and $^{40}Ar^{12}C^{++}$, $^{52}Cr^{++}$, $^{12}C^{14}N^{+}$, $^{12}C^{13}CH^{+}$ for ^{26}Mg. Unfortunately, these effects do not affect isotope analyses in the same way among different instruments and laboratories. For instance, Galy et al. (2001) and Wombacher et al. (2009) observed that Ca/Mg higher than 0.05 could induce $\delta^{26}Mg$ drifting up to +0.56‰. Teng and Yang (2014) reported smaller isotope fractionation (0.2‰) caused by the presence of Ca when the Ca/Mg increases from 0.05 to 0.3. By

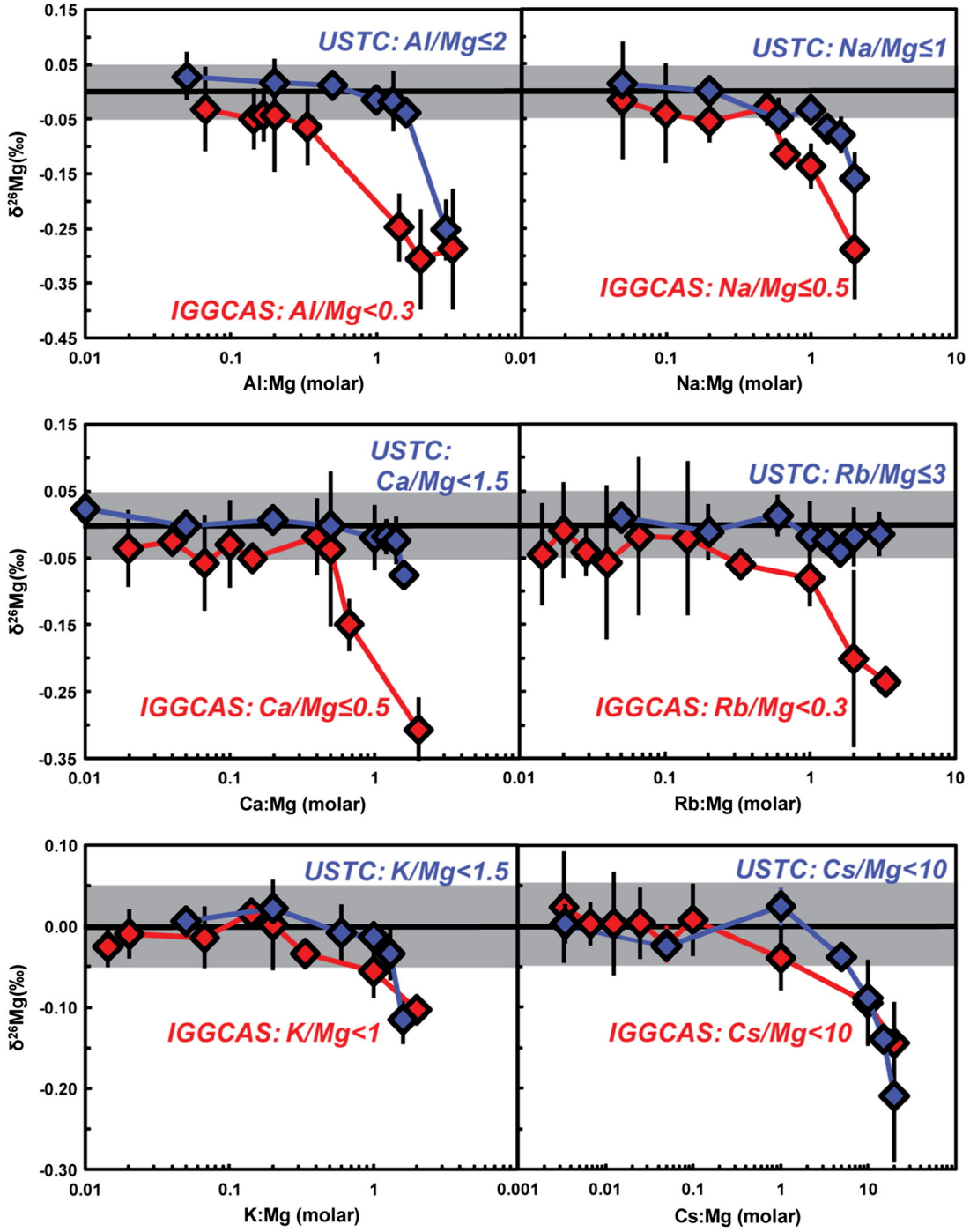

Fig. 6. Doping experiments to test matrix effect on $\delta^{26}Mg$ analyses. Mg concentrations for samples and bracketing standards (IGGMg1) are the same (2 ppm and 0.5 ppm in IGGCAS and USTC). Data are reported in Supplementary materials.

contrast, Choi et al. (2012) observed that Ca has little effect on Mg isotope measurements under cool-plasma conditions. The reason for these differences is not clear but it may be related to the running conditions of different MC-ICP-MS setups. In this study, we thoroughly tested the matrix effects on both MC-ICP-MS in the IGGCAS and USTC.

We doped an IGGMg1 solution with different proportions of Na, K, Ca, Al, Rb, and Cs to represent matrix elements that may be present in the Mg fraction chemically separated from granites and rhyolites (Fig. 6). Although it is considered as a minor element in most granitic samples, Cs was chosen for doping as it (and other minor elements) can potentially pose matrix issues in certain granitic samples with particularly high concentrations (e.g. pegmatites). While Li and Be concentrations could also be high in granites, we do not test these here as most Li and Be are removed before the Mg peak and do not affect Mg isotope analyses. The measurements on the Neptune (IGGCAS) show a negligible influence due to matrix on δ^{26}Mg when the purified samples have $^{27}Al/^{24}Mg < 0.3$, $^{23}Na/^{24}Mg \leq 0.5$, $^{39}K/^{24}Mg < 1$, $^{40}Ca/^{24}Mg \leq 0.5$, $^{85}Rb/^{24}Mg < 0.3$, and $^{133}Cs/^{24}Mg < 10$ (S-Table 1 in Supplementary materials). Although we did observe Cs in the purified Mg fractions, the maximum Cs/Mg ratio present in most of purified samples is lower than 10, which does not produce any resolvable mass bias for δ^{26}Mg based on our results.

We also found that the Neptune Plus at USTC has a higher tolerance of matrix effects than the Neptune at the IGGCAS (Fig. 6). The different responses of the two MC-ICP-MS to residual matrix elements as well as concentration mismatch mentioned above could be related to many factors, including the resolution modes (medium or low), instrumental settings (sampler cone + H-cone or Jet-cone + H-cone), different types of instruments (Neptune or Neptune plus), distinct solution concentrations, and so on. It seems that the data collected in medium resolution are more sensitive to the matrix effect than that in low resolution. At the medium resolution mode, the contributions of $^{12}C^{14}N^+$ to the measured signals of ^{26} Mg can be resolved by examining the signal peaks of blank acid solutions. Therefore, Mg isotopes were measured at the left shoulder of Mg peaks at the medium resolution mode using the Neptune MC-ICP-MS. At the low resolution mode, signal ratio of $^{26}Mg/^{12}C^{14}N^+$ is so high that the isobaric interference from $^{12}C^{14}N^+$ is negligible. In this case, Mg isotopes were measured at the center of Mg peaks.

In order to test whether our purification process decreases matrix elements below the thresholds as noted above, we compared δ^{26}Mg of the synthetic standards that passed through the column once with those that were passed through twice (Fig. 7b). After a single passage, the δ^{26}Mg of the purified solution drifted from its true value by 0.09‰. This is caused by the tail of K left in the solution (K/Mg = 2). By passing through the column a second time, all matrix cations were effectively removed so that the δ^{26}Mg of the purified solution is consistent with the recommended value within error. Similar results are also obtained for the granite standard GS-N (S-Table 2 in Supplementary materials). The δ^{26}Mg of purified solution passed through the column once differs from that passed through the column twice by 0.095‰ (−0.299 ± 0.065‰ vs. −0.204 ± 0.059‰). Therefore, we suggest performing the column chemistry procedure at least twice to acceptably separate matrix elements from Mg in low-Mg samples.

3.3. $HClO_4$ effect

In order to eliminate organic interferences inherited from samples or leached from resin, $HClO_4$ can be used to decompose organic materials in samples. Chang et al. (2003) reported that $HClO_4$ treatment of the samples after column chemistry could result in mass-dependent drift during Mg isotope analyses. Thus we also evaluated the effect of residual $HClO_4$ on Mg isotope analyses both before and after purification.

To assess fractionation that may occur before purification, we used IGGMg1 solutions mixed with different proportions of $HClO_4$ (0.5%, 2.5%, and 5%) as unknown samples. These mixed solutions passed through the column chemistry procedure, and the δ^{26}Mg of purified Mg fractions were measured using pure IGGMg1 solution as the bracketing standard. The results for the $HClO_4$-treated samples revealed no significant isotope fractionation after the column chemistry (Fig. 8). We also tested the use of 0.01 ml $HClO_4$ in digesting rock materials (RGM-1 and AGV-2), which also does not cause any measurable drift on the Mg isotope compositions (Figs. 9 and 10).

Additionally, we tested whether residual $HClO_4$ in the purified samples or $HClO_4$ added post-chemistry can affect Mg isotope analyses. For this, we measured the δ^{26}Mg of IGGMg1 doped with variable amounts of $HClO_4$. We observed that increasing $HClO_4$ in the sample will increase mass bias during the analyses (Fig. 8). Opposite to the effect of increasing HNO_3 molarities, adding 0.5% $HClO_4$ to the IGGMg1 standard caused a positive shift of the measured δ^{26}Mg by >0.11‰. On examining the results for standards treated before and after column chemistry (Fig. 8), we interpret that most of the $HClO_4$ added prior to chemistry may have been eluted early in the column procedure before Mg was eluted. Residual $HClO_4$ in the purified Mg solutions is negligible and cannot produce resolvable drift on Mg isotope measurement.

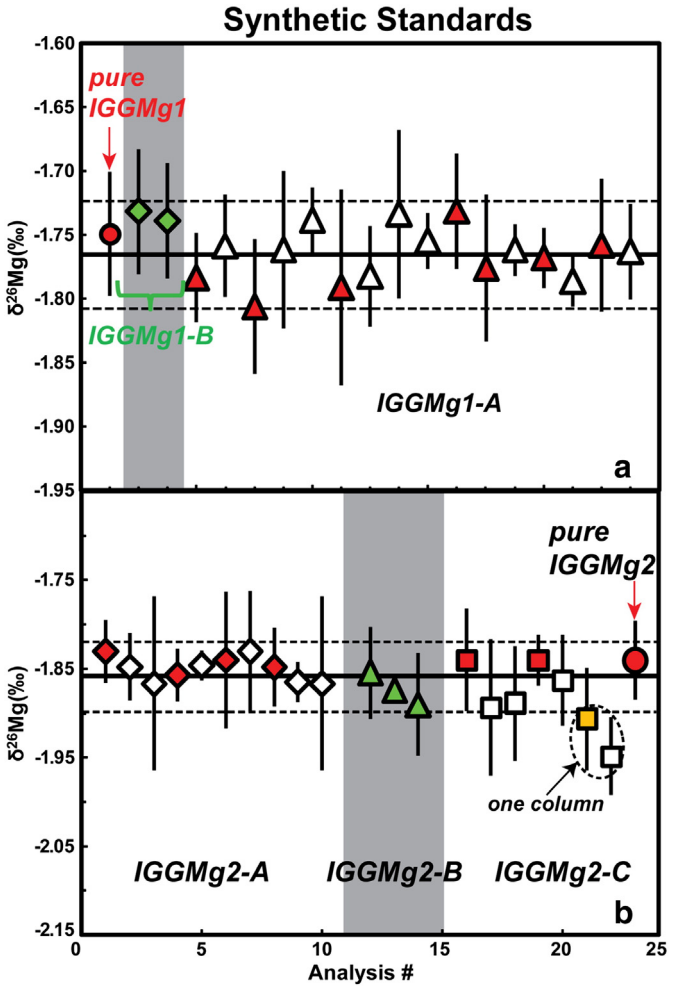

Fig. 7. Comparison of δ^{26}Mg of pure Mg standard solution relative to synthetic standards doped with Na, Fe, Ca, Al, Zn, K, Cu, Rb, and Cs. The exact elemental compositions of the doped standards can be found in Table 3. Red solid circles in both panels represent the average δ^{26}Mg for pure Mg standard solutions (IGGMg1 and IGGMg2). The bold lines represent the average δ^{26}Mg of the corresponding synthetic solutions. Note that two data points for IGGMg2-C circled by a dashed line at right are the δ^{26}Mg for the synthetic solution with only one column purification (Fig. 7b). All other doped IGGMg standards were passed through the columns twice. (For interpretation of the references to color in this figure legend, the reader is referred to the web version of this article.)

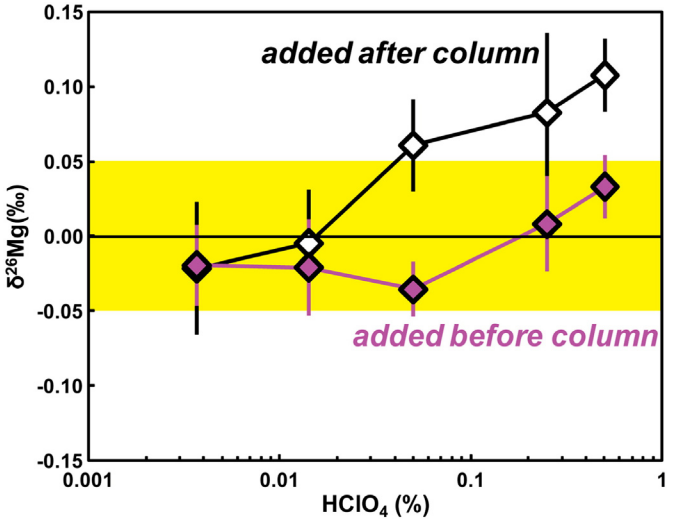

Fig. 8. $HClO_4$ effect on $\delta^{26}Mg$ for IGGMg1 standard solutions with and without chemical purification. The solid diamonds show $\delta^{26}Mg$ of IGGMg1 pre-treated with $HClO_4$ which passed through the column chemistry. The open diamonds are $\delta^{26}Mg$ of IGGMg1 + $HClO_4$ without passing through the column.

3.4. Precision and accuracy

Precision and accuracy of our method were assessed by conducting replicated measurements of pure Mg standards, synthetic standards, and rock standards. These duplicates include independent digestion of the same rock powder, repeated purification of the same bulk raw solution, and measurements of the same purified solutions on different days. Results for these duplicates are listed in the Supplementary Materials. Additionally, a large number of mono-elemental and rock standards were repeatedly measured using both the Neptune at IGGCAS and the Neptune Plus at USTC (Figs. 10–12). The results from the two laboratories agreed well with each other within the uncertainty, further ensuring the quality of the data.

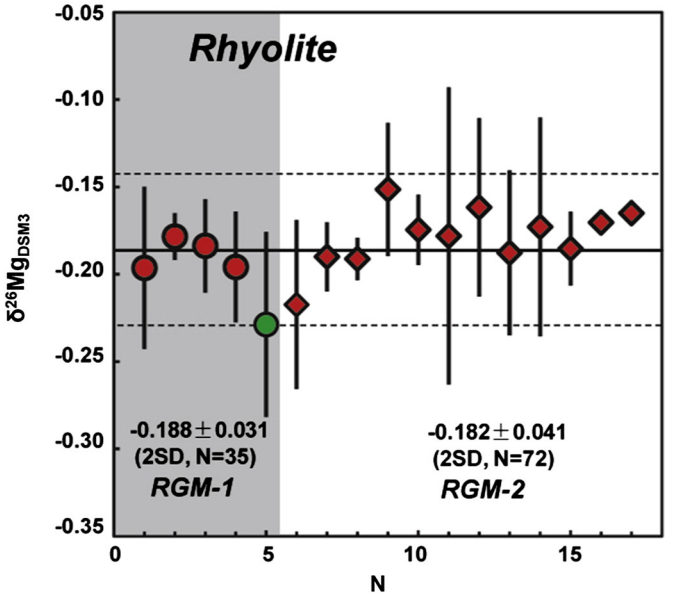

Fig. 9. $\delta^{26}Mg$ of rhyolite standards RGM-1 and RGM-2. The red circles denote RGM-1, and the red diamonds denote RGM-2. The green circle represents $\delta^{26}Mg$ of RGM-1 with $HClO_4$ treatment. Each symbol denotes an independent measurement (from powder digestion to isotope analyses). (For interpretation of the references to color in this figure legend, the reader is referred to the web version of this article.)

The accuracy of our method was shown through measurement of two synthetic standards made by mixing mono-elemental Mg standards (IGGMg1 and IGGMg2) with a number of matrix elements. IGGMg1 and IGGMg2 are characterized by $\delta^{26}Mg$ of $-1.746 \pm 0.047‰$ and $-1.840 \pm 0.044‰$, respectively. IGGMg1-A has concentration ratios of K: Al: Fe: Na: Ca: Mg: Mn: Rb: Ti: Zn: Cs: Cu of 20: 10: 8: 5: 5: 1: 1: 0.2: 0.1: 0.02: 0.01: 0.01. IGGMg1-B is the pure IGGMg1 standard after passing through the column chemistry procedure. After purification, the standard solutions (IGGMg1-A of $-1.766 \pm 0.042‰$, and IGGMg1-B of $-1.735 \pm 0.010‰$) yield indistinguishable $\delta^{26}Mg$ from the pure IGGMg1, within analytical uncertainty (Fig. 7a). IGGMg2-A is the mixture of standard IGGMg2 with the matrix elements and concentrations found in the standard RGM-1. IGGMg2-B and IGGMg2-C are the mixtures of IGGMg2 with different matrices including K, Al, Fe, Na, Ca, Mg, Mn, Rb, Ti, Zn, Cs, and Cu (Table 3). Following the purification routine and analytical methods described previously, our measurement does not show any significant difference in $\delta^{26}Mg$ between the pure IGGMg2 and synthetic solutions (such as IGGMg2-A of $-1.850 \pm 0.028‰$, IGGMg2-B of $-1.873 \pm 0.036‰$, and IGGMg2-C of $-1.865 \pm 0.051‰$) (Fig. 7b). It verifies that purification procedure and MC-ICP-MS measurement developed in this study are robust and reproducible with excellent accuracy.

The long-term external precision was evaluated by repeated analyses of the international Mg standards (DSM-3 and CAM-1), in-house Mg standards (IGGMg1, IGGMg2, and SRM980), and igneous rock standards. The in-run precision on the $^{26}Mg/^{24}Mg$ ratio for a single measurement of one 60-ratio block is $\leq 0.02‰$ for both MC-ICP-MS. The internal precision on the measured $^{26}Mg/^{24}Mg$, based on ≥ 4 repeated runs of the same solution during a single analytical session, is $\leq 0.05‰$ (2σ) in both laboratories. Long-term analyses of the IGGMg1 standard over ten months produced a total average $\delta^{26}Mg$ of $-1.746 \pm 0.047‰$ (2σ; n = 125), with similar $\delta^{26}Mg$ of $-1.742 \pm 0.041‰$ (2σ; n = 53) and $-1.749 \pm 0.049‰$ (2σ; n = 72) in the IGGCAS and USTC, respectively. NIST standard SRM980 were $-2.840 \pm 0.043‰$ (2σ, n = 70) and $-2.823 \pm 0.052‰$ (2σ, n = 62), respectively. CAM-1 has $\delta^{26}Mg$ of $-2.597 \pm 0.042‰$ (2σ, n = 49) and $-2.598 \pm 0.039‰$ (2σ, n = 70) in the two laboratories, with a total average $\delta^{26}Mg$ of $-2.598 \pm 0.040‰$ (2σ, n = 119) (Fig. 11). These are in agreement with published values ($\delta^{26}Mg = -2.607 \pm 0.050‰$, n = 2387) (see (An and Huang, 2014) and references therein).

Seven total procedural replicates of synthetic standard IGGMg1-A (from column chemistry to measurement) conducted over the course of this study yielded an average $\delta^{26}Mg$ of $-1.766‰ \pm 0.042$ (2σ, n = 53), consistent with the expected value of $-1.749 \pm 0.049‰$ (2σ, n = 72) for the pure IGGMg1 standard. A magnesium three-isotope plot of all rock materials and the Mg standards defines a single fractionation line with a slope of 0.518 ± 0.001 (Fig. 13), consistent with the theoretical values for equilibrium and kinetic fractionation of 0.521 and 0.510, respectively (Young et al., 2002; Young and Galy, 2004).

3.5. $\delta^{26}Mg$ of reference materials

Using the method developed here, we measured sixteen widely-used rock standards with large variations in major elements (S-Table 2 in Supplementary materials). There are many fewer studies of the Mg isotope compositions of granite and rhyolite standards than for basalt standards (Bolou-Bi et al., 2009; Huang et al., 2009b; Li et al., 2010), and this is the first report of $\delta^{26}Mg$ for rhyolite standards (RGM-1 and RGM-2). RGM-1 has an average $\delta^{26}Mg$ of $-0.188 \pm 0.031‰$ (2σ, n = 35). The second rhyolite standard obtained from the same rock body (RGM-2) has a similar $\delta^{26}Mg$ of $-0.182 \pm 0.041‰$ (2σ, n = 72), slightly heavier than the mantle value (Teng et al., 2007, 2010a; Huang et al., 2009b; Yang et al., 2009; Young et al., 2009; Bourdon et al., 2010; Chakrabarti and Jacobsen, 2010). Our results suggest no measurable difference in $\delta^{26}Mg$ between RGM-1 and RGM-2 (Fig. 9).

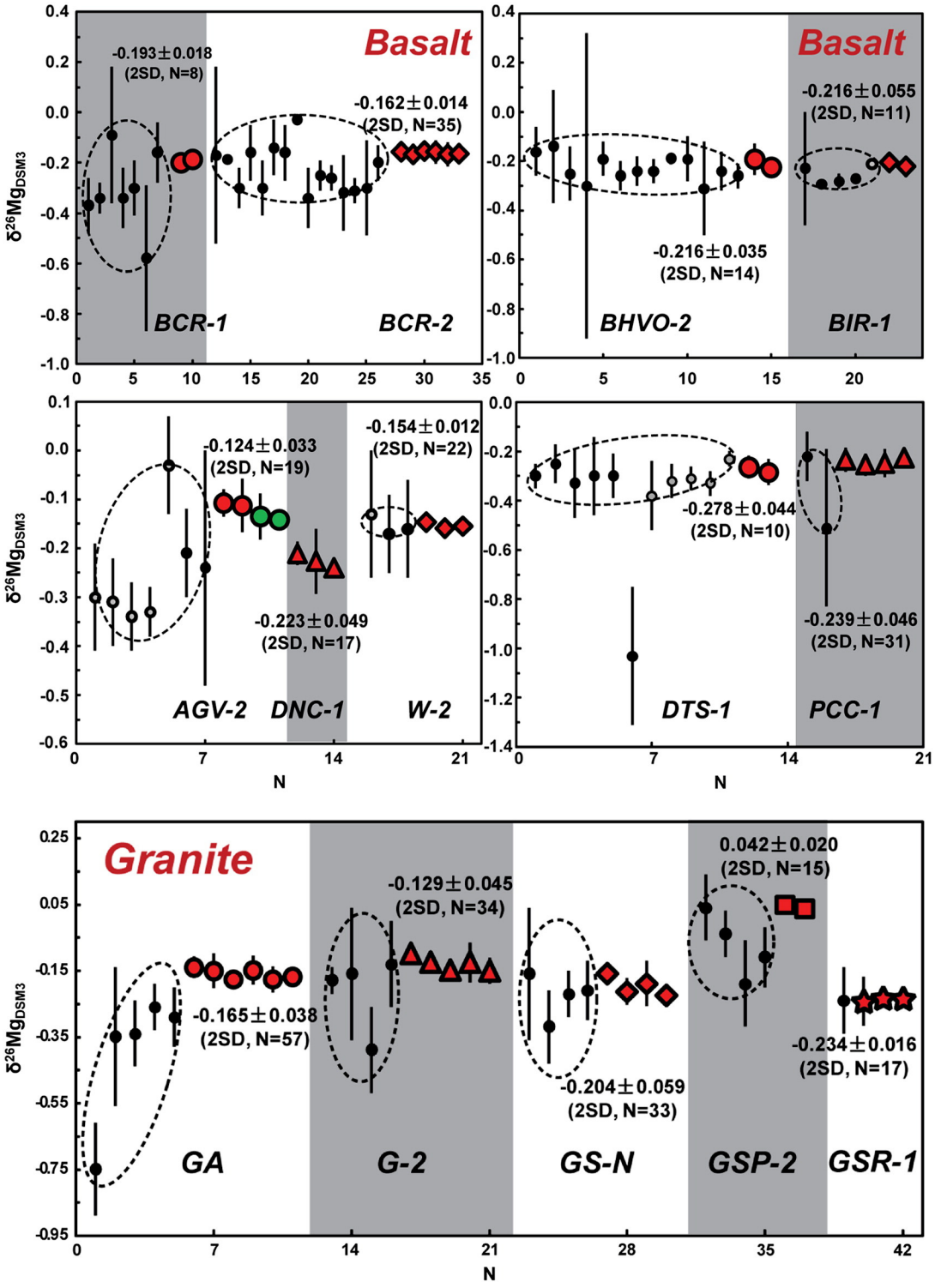

Fig. 10. Long-term δ^{26}Mg analyses of silicate rock standards with various rock types and MgO contents (Table 4), including the data from this study and previous studies. Small black circles represent literature data, and colorful symbols represent the data from this study. Errors of data from the literature and this study reflect 2 standard deviations (2σ). The two green circles represent Mg isotope data for AGV-2 with $HClO_4$ pre-treatment. The small gray circles represent published data for AGV-1 while the black ones stand for AGV-2; similarly, the small black and gray circles represent that for DTS-1 and DTS-2, respectively.

We provide δ^{26}Mg data for five granite standards (GA, G-2, GS-N, GSP-2, and GSR-1), that show consistency with most previous work within uncertainties (Fig. 10). The δ^{26}Mg of the granite standard GA in this study is −0.165 ± 0.038‰ (2σ, n = 57), consistent with literature values within error (−0.34 ± 0.15‰ (Huang et al., 2009b) and −0.26 ± 0.07‰ (Li et al., 2010)), but it is significantly heavier than one reported value (−0.75 ± 0.14‰ (Bolou-Bi et al., 2009)). The average δ^{26}Mg of G-2 is −0.129 ± 0.045‰ (2σ, n = 34), in agreement with literature values (−0.18 ± 0.04‰, −0.16 ± 0.20‰, and −0.13 ± 0.13‰ (Huang et al., 2009b)). The δ^{26}Mg of GSP-2 is −0.042 ± 0.020‰ (2σ, n = 15), and GSR-1 is −0.234 ± 0.016‰ (2σ, n = 17). Both are consistent with reported values in the literature

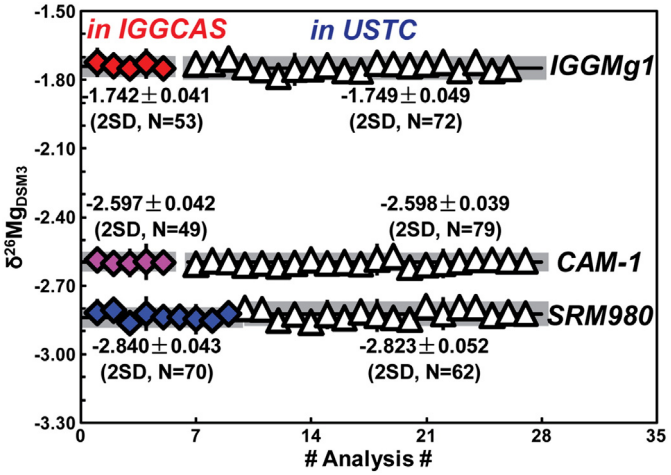

Fig. 11. δ^{26}Mg of CAM-1, SRM980, and in-house Mg standard solution IGGMg1. The long-term external precision is better than ±0.05‰ (2σ).

within error (Huang et al., 2009b; Wang et al., 2011). GS-N has an average δ^{26}Mg of −0.204 ± 0.059‰ (2σ, n = 33), identical with the published data (−0.24 ± 0.23‰ (Huang et al., 2009b), −0.22 ± 0.07 and −0.21 ± 0.09‰ (Li et al., 2010)).

We also analyzed high-Mg standards including andesites, basalts, diabase, dolerite, and peridotites at both IGGCAS and USTC (Figs. 10 and 12). The δ^{26}Mg of W-2 was −0.154 ± 0.012‰ (2σ, n = 22), which was consistent with published values within error (Huang et al., 2009b; Wang et al., 2011; Choi et al., 2012). Similarly, the δ^{26}Mg of AGV-2 was −0.124 ± 0.033‰ (2σ, n = 19) and identical to reported values within error (Choi et al., 2012; Opfergelt et al., 2012). The δ^{26}Mg of DNC-1 was −0.223 ± 0.049‰ (2σ, n = 17) and no data has yet been reported in previous studies for this dolerite standard. The δ^{26}Mg of Columbia River basalt standard (BCR-1) was −0.193 ± 0.018‰ (2σ, n = 8) and BCR-2 was −0.162 ± 0.014‰ (2σ, n = 35). These δ^{26}Mg values were in agreement within uncertainty with some reported values such as −0.16 ± 0.11‰ (Bourdon et al., 2010), −0.19 ± 0.02 (Baker et al., 2005), −0.17 ± 0.35‰ (Bizzarro et al., 2004), −0.14 ± 0.11‰ (Wombacher et al., 2009), −0.16 ± 0.11 (Tipper et al., 2008a), −0.25 ± 0.06‰ (Pogge von Strandmann et al., 2011), and −0.20 ± 0.07‰ (Wimpenny et al., 2014b), but slightly heavier than other values such as −0.30 ± 0.11‰ (Huang et al., 2009b), −0.30 ± 0.08‰

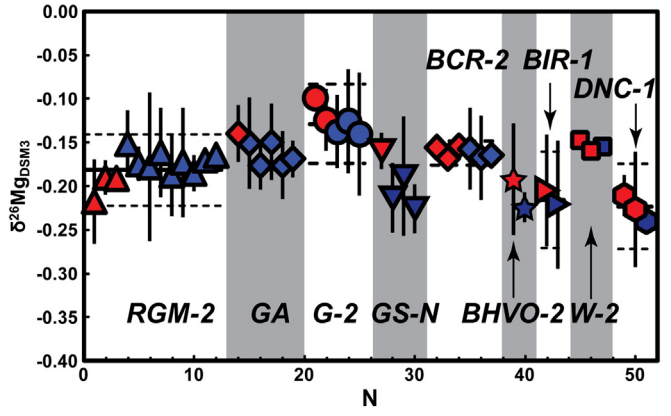

Fig. 12. Comparisons of Mg isotopic compositions of rock standards measured at IGGCAS and USTC. Red symbols are from the IGGCAS; blue symbols are from USTC. Sample shapes represent each labeled standard measured (i.e. G-2 are represented by circles). The rock types and MgO contents of these standards are listed in Table 4. (For interpretation of the references to color in this figure legend, the reader is referred to the web version of this article.)

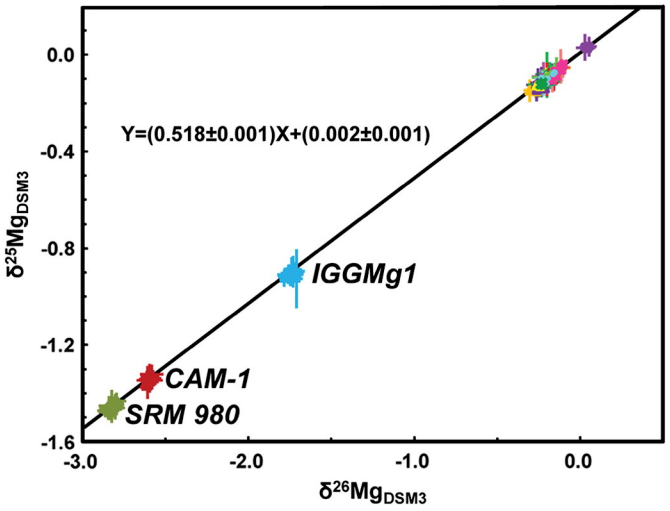

Fig. 13. Magnesium three isotope plot of all standards and samples analyzed in this study defines a line with a slope of 0.518 ± 0.001, close to the theoretical equilibrium and kinetic fractionation values for Mg isotopes (0.521 and 0.510, respectively) (Young et al., 2002).

(Teng et al., 2007), −0.32 ± 0.15‰ (Bouvier et al., 2013), and −0.31 ± 0.05‰ (Choi et al., 2012). Clearly, there are significant inter-laboratory discrepancies for some standards (e.g., BCR-2 and GA). The reason for such discrepancy is not clear, but it is more likely due to analytical artifacts caused by different purification procedures or sample introduction systems (e.g., "wet" vs. "dry" plasma conditions). For example, the relatively large uncertainty of δ^{26}Mg for low-MgO granites in previous studies (e.g., Huang et al., 2009b) may be related to measurement of a diluted solution (~0.2 ppm) using the "dry" plasma method which may be easily affected by the residual matrix in the Mg solution (Huang et al., 2009b). Also as suggested in Teng and Yang (2014), analyses using "dry" plasma are more sensitive to both the matrix effect and concentration mismatch than those using "wet" plasma.

Basalt standards BHVO-2 and BIR-1 have similar Mg isotope compositions of −0.216 ± 0.035‰ (2σ, n = 14), and −0.216 ± 0.055‰ (2σ, n = 11), respectively, consistent with previous studies (Pogge von Strandmann et al., 2008, 2011; Wombacher et al., 2009; Bizzarro et al., 2011; Huang et al., 2012). The average δ^{26}Mg of PCC-1 is −0.239 ± 0.046‰ (2σ, n = 31), consistent with the literature value (−0.22 ± 0.10‰) (Huang et al., 2009b). The overall δ^{26}Mg for igneous rock standards analyzed in this study ranges from −0.278‰ to −0.042‰. Dunite standard DTS-1 has the lightest Mg isotope composition (−0.278 ± 0.044‰) among all geostandards analyzed, while GSP-2 has the heaviest value (0.042 ± 0.020‰).

4. Applications

Many low-Mg rocks (MgO <1 wt.%) have important geological implications. For instance, granites constitute the most voluminous lithological units in the upper continental crust. Previous studies have reported relatively homogeneous δ^{26}Mg of I-type (−0.25‰ to −0.15‰) and S-type (−0.23‰ to −0.14‰) granites which may reflect the signature of their crustal sources, while the substantial variation in A-type granites (−0.28‰–+0.34‰) was ascribed to source heterogeneity (Li et al., 2010; Liu et al., 2010). Thus Mg isotopes can be used to further constrain granite genesis. In some previous studies, the δ^{26}Mg value of a whole-rock granite sample was represented by analysis of only the mafic minerals in the rocks (Shen et al., 2009; Liu et al., 2010). Our procedure developed and presented here provides a direct and fast way to analyze δ^{26}Mg of the whole rock, which is especially useful for samples without Mg-rich mafic minerals, such as rhyolites, loess, and low-Mg carbonatites.

Table 4
Mg isotope compositions of igneous rock standards reported in this study.

Standard	MgO (wt.%)	δ^{26}Mg	2SD	δ^{25}Mg	2SD	δ^{26}Mg/δ^{25}Mg	n
Rhyolite							
RGM-1	0.28	−0.188	0.031	−0.092	0.017	2.039	35
RGM-1 ($HClO_4$)		−0.229	0.053	−0.113	0.029	2.023	8
RGM-2	0.28	−0.182	0.041	−0.091	0.027	1.992	72
Average of RGM		−0.184	0.038	−0.092	0.024	2.007	107
Average of RGM (includes added $HClO_4$)		−0.186	0.043	−0.093	0.026	2.008	115
Granite							
GSR-1	0.42	−0.234	0.016	−0.123	0.011	1.908	17
G-2	0.75	−0.129	0.045	−0.067	0.044	1.916	34
GA	0.95	−0.165	0.038	−0.084	0.027	1.954	57
GS-N	2.30	−0.204	0.059	−0.107	0.036	1.914	33
Granodiorite							
GSP-2	0.96	0.042	0.020	0.030	0.011	1.377	15
Andesite							
AGV-2	1.79	−0.110	0.007	−0.051	0.013	2.182	11
AGV-2 ($HClO_4$)		−0.138	0.010	−0.070	0.019	1.980	8
Average of AGV-2 (includes added $HClO_4$)		−0.124	0.033	−0.060	0.026	2.065	19
Basalt							
BCR-1	2.16	−0.193	0.018	−0.100	0.008	1.936	8
BCR-2	2.16	−0.162	0.014	−0.082	0.021	1.968	35
Average of BCR		−0.168	0.029	−0.085	0.023	1.961	43
BHVO-2	7.23	−0.216	0.035	−0.102	0.030	2.124	14
BIR-1	9.70	−0.216	0.055	−0.104	0.023	2.070	11
Diabase							
W-2	6.37	−0.154	0.012	−0.077	0.019	1.996	22
DNC-1	10.13	−0.223	0.049	−0.111	0.029	2.018	17
Peridotite							
PCC-1	44.43	−0.239	0.046	−0.123	0.026	1.938	31
DTS-1	49.40	−0.278	0.044	−0.150	0.003	1.850	10

n represents the total number of repeated runs of all solutions during different analytical sessions, including the same purified solutions and large amounts of total procedural replicates.

Furthermore, the long-term external precision of our method is better than ±0.05‰ (2σ) for δ^{26}Mg based on replicated analyses of rock and synthetic standards. Although the method is designed for low-Mg samples, it can also be applied to the more commonly performed high-Mg rock and mineral measurements. This provides a stepping stone to more accurately determine the slight fractionation of Mg isotopes found in high-temperature terrestrial samples and mantle minerals.

With our new procedure, we revisited mineral separates from peridotite xenoliths from Lianshan (LHLS) measured in a previous study with a published error of 0.05‰/amu (2σ) (Huang et al., 2011) (Table 5). We present high-precision Mg isotope compositions of olivine, orthopyroxene (opx), and clinopyroxene (cpx) for 5 lherzolite xenoliths. $\triangle^{26}Mg_{ol\text{-}cpx}$ of sample LHLS6 varied from −0.093‰ to −0.104‰ with an average value of −0.098 ± 0.051‰ (2σ, n = 12). These offsets agreed well with the reported values of mantle minerals (Handler et al., 2009; Huang et al., 2009b; Yang et al., 2009; Young et al., 2009), and the theoretical prediction for inter-mineral equilibrium fractionation at high temperatures (Young et al., 2009; Schauble, 2011; Huang et al., 2013). With the excellent precision of our method, we can resolve the slight fractionation between olivines from different mantle xenoliths, such as LHLS5 olivine (−0.338 ± 0.042‰) and LHLS6 olivine (−0.209 ± 0.021‰), which is helpful for better understanding Mg isotope fractionation in the mantle caused by metasomatism and diffusion (Huang et al., 2011; Xiao et al., 2013). Finally, an improved precision can also decrease the uncertainty of temperature estimates using Mg isotope thermometry (Li et al., 2011; Huang et al., 2013).

5. Conclusions

In this paper, we presented a new method to obtain precise and accurate Mg isotope compositions for rocks that contain small amounts of Mg (MgO < 1 wt.%). By adding a trace amount of HF to the eluting acid, we greatly improve the separation efficiency of Mg from matrix elements common to low-Mg rocks, such as Ti, Al, Fe, and K. We systematically tested and rigorously examined all of the common parameters that could affect the precision and accuracy of Mg isotope analyses, including matrix effects, Mg concentration mismatch between samples and standards during MC-ICP-MS analysis, acid molarity mismatch between sample and standard solutions during analysis, and the isotopic fractionation that can be caused by the use of $HClO_4$. As long as a purified sample contains ratios of $^{27}Al/^{24}Mg$ <0.3, $^{23}Na/^{24}Mg$ ≤0.5, $^{39}K/^{24}Mg$ <1, $^{40}Ca/^{24}Mg$ ≤0.5, $^{85}Rb/^{24}Mg$ <0.3, and $^{133}Cs/^{24}Mg$ <10, we demonstrate that δ^{26}Mg is not measurably affected by matrix elements. Significant errors can occur when the difference of sample-standard Mg concentrations is >20%, the analytical dilution acid molarities are different by >25%, and the $HClO_4$ molarity of samples is >0.5% at the time of analysis. Using our method, we obtained δ^{26}Mg for rhyolite standard RGM-1 (−0.188 ± 0.031‰) and RGM-2 (−0.182 ± 0.041‰). The δ^{26}Mg of granite standard GA is −0.165 ± 0.038‰ (2σ, n = 57), G-2 is −0.129 ± 0.045‰ (2σ, n = 34), GS-N is −0.204 ± 0.059‰ (2σ, n = 33), GSP-2 is −0.042 ± 0.020‰ (2σ, n = 15), and GSR-1 is −0.234 ± 0.016‰ (2σ, n = 17). Based on a number of standard analyses, the long-term external precision is better than ±0.05‰ (2σ). Such precision allows us to identify the slight fractionation of Mg isotopes in high-temperature terrestrial samples. With our method, Mg isotopes can be more widely used to study geochemical processes in low-Mg rocks as well as many high-Mg rocks.

Table 5
Re-analyzed Mg isotope data for mantle minerals.
The literature values are from Huang et al. (2011).

Sample		Olivine					Orthopyroxene					Clinopyroxene					$\triangle^{26}Mg_{ol\text{-}cpx}$	2SD
		δ^{26}Mg	2SD	δ^{25}Mg	2SD	n	δ^{26}Mg	2SD	δ^{25}Mg	2SD	n	δ^{26}Mg	2SD	δ^{26}Mg	2SD	n		
LHLS1	This study						−0.233	0.049	−0.114	0.025	6							
	Literature data						−0.34	0.08	−0.19	0.07	8							
LHLS4	This study											−0.215	0.042	−0.112	0.041	6		
	Literature data											−0.43	0.04	−0.24	0.04	4		
LHLS5	This study	−0.338	0.042	−0.173	0.026	6												
	This study	−0.329	0.066	−0.177	0.048	6												
	Literature data	−0.42	0.10	−0.23	0.06	8												
LHLS6	This study	−0.209	0.021	−0.115	0.016	6						−0.105	0.027	−0.057	0.034	6	−0.098	0.051
	This study											−0.116	0.051	−0.062	0.035	6		
	Literature data	−0.25	0.10	−0.10	0.08	9						−0.09	0.10	−0.05	0.05	4	−0.15	0.14
LHLS10	This study						−0.236	0.029	−0.121	0.025	6							
	Literature data						−0.19	0.12	−0.09	0.08	6							

Acknowledgments

We thank A. Galy for providing DSM-3 and CAM-1 standard solutions. This work is supported by the National Science Foundation of China (41173031, 41325011, and 40873009), the 111 Project, the Fundamental Research Funds for the Central Universities, and the SKL1301 project of the State Key Laboratory of Lithospheric Evolution, Institute of Geology and Geophysics, Chinese Academy of Sciences. We are thankful for the constructive comments on drafts by A. Galy, and the editorial help and comments by L. Reisberg.

Appendix A. Supplementary data

Supplementary data to this article can be found online at http://dx.doi.org/10.1016/j.chemgeo.2014.09.014.

References

An, Y., Huang, F., 2014. A review of Mg isotope analytical methods by MC-ICP-MS. J. Earth Sci. 25, 822–840.
Baker, J., Bizzarro, M., Wittig, N., Connelly, J., Haack, H., 2005. Early planetesimal melting from an age of 4.5662 Gyr for differentiated meteorites. Nature 436 (7054), 1127–1131.
Bizzarro, M., Baker, J.A., Haack, H., 2004. Mg isotope evidence for contemporaneous formation of chondrules and refractory inclusions. Nature 431 (7006), 275–278.
Bizzarro, M., Paton, C., Larsen, K., Schiller, M., Trinquier, A., Ulfbeck, D., 2011. High-precision Mg-isotope measurements of terrestrial and extraterrestrial material by HR-MC-ICPMS-implications for the relative and absolute Mg-isotope composition of the bulk silicate Earth. J. Anal. At. Spectrom. 26 (3), 565–577.
Black, J.R., Yin, Q.-z, Casey, W.H., 2006. An experimental study of magnesium-isotope fractionation in chlorophyll-a photosynthesis. Geochim. Cosmochim. Acta 70 (16), 4072–4079.
Black, J.R., John, S., Young, E.D., Kavner, A., 2010. Effect of temperature and mass transport on transition metal isotope fractionation during electroplating. Geochim. Cosmochim. Acta 74 (18), 5187–5201.
Bolou-Bi, E.B., Vigier, N., Brenot, A., Poszwa, A., 2009. Magnesium isotope compositions of natural reference materials. Geostand. Geoanal. Res. 33 (1), 95–109.
Bourdon, B., Tipper, E.T., Fitoussi, C., Stracke, A., 2010. Chondritic Mg isotope composition of the Earth. Geochim. Cosmochim. Acta 74 (17), 5069–5083.
Bouvier, A., Wadhwa, M., Simon, S.B., Grossman, L., 2013. Magnesium isotopic fractionation in chondrules from the Murchison and Murray CM2 carbonaceous chondrites. Meteorit. Planet. Sci. 1–15.
Brenot, A., Cloquet, C., Vigier, N., Carignan, J., France-Lanord, C., 2008. Magnesium isotope systematics of the lithologically varied Moselle river basin, France. Geochim. Cosmochim. Acta 72 (20), 5070–5089.
Buhl, D., Immenhauser, A., Smeulders, G., Kabiri, L., Richter, D.K., 2007. Time series δ^{26}Mg analysis in speleothem calcite: Kinetic versus equilibrium fractionation, comparison with other proxies and implications for palaeoclimate research. Chem. Geol. 244 (3–4), 715–729.
Chakrabarti, R., Jacobsen, S.B., 2010. The isotopic composition of magnesium in the inner Solar System. Earth Planet. Sci. Lett. 293 (3–4), 349–358.
Chang, V.T.C., Makishima, A., Belshaw, N.S., O'Nions, R.K., 2003. Purification of Mg from low-Mg biogenic carbonates for isotope ratio determination using multiple collector ICP-MS. J. Anal. At. Spectrom. 18 (4), 296–301.
Chang, V.T.C., Williams, R.J.P., Makishima, A., Belshawl, N.S., O'Nions, R.K., 2004. Mg and Ca isotope fractionation during $CaCO_3$ biomineralisation. Biochem. Biophys. Res. Commun. 323 (1), 79–85.
Choi, M.S., Ryu, J.-S., Lee, S.-W., Shin, H.S., Lee, K.-S., 2012. A revisited method for Mg purification and isotope analysis using cool-plasma MC-ICP-MS. J. Anal. At. Spectrom. 27 (11), 1955–1959.
Foster, G.L., Pogge von Strandmann, P.A.E., Rae, J.W.B., 2010. Boron and magnesium isotopic composition of seawater. Geochem. Geophys. Geosyst. 11 (8), Q08015.
Fritz, J.S., Garralda, B.B., Karraker, S.K., 1961. Cation exchange separation of metla ions by elution with hydrofluoric acid. Anal. Chim. Acta. 33, 882–886.
Galy, A., Young, E.D., Ash, R.D., Keith O'Nions, R., 2000. The formation of chondrules at high gas pressures in the solar nebula. Science 290 (5497), 1751–1753.
Galy, A., Belshaw, N.S., Halicz, L., O'Nions, R.K., 2001. High-precision measurement of magnesium isotopes by multiple-collector inductively coupled plasma mass spectrometry. Int. J. Mass Spectrom. 208 (1–3), 89–98.
Galy, A., Bar-Matthews, M., Halicz, L., O'Nions, R.K., 2002. Mg isotopic composition of carbonate: insight from speleothem formation. Earth Planet. Sci. Lett. 201 (1), 105–115.
Galy, A., Yoffe, O., Janney, P.E., Williams, R.W., Cloquet, C., Alard, O., Halicz, L., Wadhwa, M., Hutcheon, I.D., Ramon, E., Carignan, J., 2003. Magnesium isotope heterogeneity of the isotopic standard SRM980 and new reference materials for magnesium-isotope-ratio measurements. J. Anal. At. Spectrom. 18 (11), 1352–1356.
Handler, M.R., Baker, J.A., Schiller, M., Bennett, V.C., Yaxley, G.M., 2009. Magnesium stable isotope composition of Earth's upper mantle. Earth Planet. Sci. Lett. 282 (1–4), 306–313.
Higgins, J.A., Schrag, D.P., 2010. Constraining magnesium cycling in marine sediments using magnesium isotopes. Geochim. Cosmochim. Acta 74 (17), 5039–5053.
Hippler, D., Buhl, D., Witbaard, R., Richter, D.K., Immenhauser, A., 2009. Towards a better understanding of magnesium-isotope ratios from marine skeletal carbonates. Geochim. Cosmochim. Acta 73 (20), 6134–6146.
Huang, F., Glessner, J., Ianno, A., Lundstrom, C., Zhang, Z., 2009a. Magnesium isotopic composition of igneous rock standards measured by MC-ICP-MS. Chem. Geol. 268 (1–2), 15–23.
Huang, F., Lundstrom, C.C., Glessner, J., Ianno, A., Boudreau, A., Li, J., Ferré, E.C., Marshak, S., DeFrates, J., 2009b. Chemical and isotopic fractionation of wet andesite in a temperature gradient: experiments and models suggesting a new mechanism of magma differentiation. Geochim. Cosmochim. Acta 73 (3), 729–749.
Huang, F., Zhang, Z., Lundstrom, C.C., Zhi, X., 2011. Iron and magnesium isotopic compositions of peridotite xenoliths from Eastern China. Geochim. Cosmochim. Acta 75 (12), 3318–3334.
Huang, K.-J., Teng, F.-Z., Wei, G.-J., Ma, J.-L., Bao, Z.-Y., 2012. Adsorption- and desorption-controlled magnesium isotope fractionation during extreme weathering of basalt in Hainan Island, China. Earth Planet. Sci. Lett. 359–360, 73–83.
Huang, F., Chen, L., Wu, Z., Wang, W., 2013. First-principles calculations of equilibrium Mg isotope fractionations between garnet, clinopyroxene, orthopyroxene, and olivine: Implications for Mg isotope thermometry. Earth Planet. Sci. Lett. 367, 61–70.
Lee, T., Papanastassiou, D.A., 1974. Mg isotopic anomalies in the Allende Meteorite and correlation with O and Sr effects. Geophys. Res. Lett. 1, 225–228.
Li, W.-Y., Teng, F.-Z., Ke, S., Rudnick, R.L., Gao, S., Wu, F.-Y., Chappell, B.W., 2010. Heterogeneous magnesium isotopic composition of the upper continental crust. Geochim. Cosmochim. Acta 74 (23), 6867–6884.
Li, W.-Y., Teng, F.-Z., Xiao, Y., Huang, J., 2011. High-temperature inter-mineral magnesium isotope fractionation in eclogite from the Dabie orogen. China. Earth Planet. Sci. Lett. 304, 224–230.
Liu, S.-A., Teng, F.-Z., He, Y., Ke, S., Li, S., 2010. Investigation of magnesium isotope fractionation during granite differentiation: implication for Mg isotopic composition of the continental crust. Earth Planet. Sci. Lett. 297 (3–4), 646–654.
Liu, S.-A., Teng, F.-Z., Yang, W., Wu, F.-Y., 2011. High-temperature inter-mineral magnesium isotope fractionation in mantle xenoliths from the North China craton. Earth Planet. Sci. Lett. 308 (1–2), 131–140.
Liu, S.-A., Li, D., Li, S., Teng, F.-Z., Ke, S., He, Y., Lu, Y., 2014. High-precision copper and iron isotope analysis of igneous rock standards by MC-ICP-MS. J. Anal. At. Spectrom. 29 (1), 122–133.
Malinovsky, D., Stenberg, A., Rodushkin, I., Andren, H., Ingri, J., Ohlander, B., Baxter, D.C., 2003. Performance of high resolution MC-ICP-MS for Fe isotope ratio measurements in sedimentary geological materials. J. Anal. At. Spectrom. 18 (7), 687–695.
McDonough, W.F., Sun, S.s, 1995. The composition of the Earth. Chem. Geol. 120 (3–4), 223–253.
Millero, F.J., 1974. The physical chemistry of seawater. Annu. Rev. Earth Planet. Sci. 2 (1), 101–150.
Opfergelt, S., Georg, R.B., Delvaux, B., Cabidoche, Y.M., Burton, K.W., Halliday, A.N., 2012. Mechanisms of magnesium isotope fractionation in volcanic soil weathering sequences, Guadeloupe. Earth Planet. Sci. Lett. 341–344, 176–185.
Pearson, N.J., Griffin, W.L., Alard, O., O'Reilly, S.Y., 2006. The isotopic composition of magnesium in mantle olivine: records of depletion and metasomatism. Chem. Geol. 226 (3–4), 115–133.
Pogge von Strandmann, P.A.E., 2008. Precise magnesium isotope measurements in core top planktic and benthic foraminifera. Geochem. Geophys. Geosyst. 9 (12), Q12015.
Pogge von Strandmann, P.A.E., James, R.H., van Calsteren, P., Gíslason, S.R., Burton, K.W., 2008. Lithium, magnesium and uranium isotope behaviour in the estuarine environment of basaltic islands. Earth Planet. Sci. Lett. 274 (3–4), 462–471.
Pogge von Strandmann, P.A.E., Elliott, T., Marschall, H.R., Coath, C., Lai, Y.-J., Jeffcoate, A.B., Ionov, D.A., 2011. Variations of Li and Mg isotope ratios in bulk chondrites and mantle xenoliths. Geochim. Cosmochim. Acta 75 (18), 5247–5268.
Richter, F.M., Watson, E.B., Mendybaev, R.A., Teng, F.-Z., Janney, P.E., 2008. Magnesium isotope fractionation in silicate melts by chemical and thermal diffusion. Geochim. Cosmochim. Acta 72 (1), 206–220.
Rudnick, R.L., 2003. Composition of the continental crust. In: Rudnick, R.L. (Ed.), The Crust. In: Holland, H.D., Turekian, K.K. (Eds.), vol. 3. Elsevier-Pergamon, Oxford, pp. 1–64.
Schauble, E.A., 2011. First-principles estimates of equilibrium magnesium isotope fractionation in silicate, oxide, carbonate and hexaaquamagnesium(2+) crystals. Geochim. Cosmochim. Acta 75 (3), 844–869.
Schiller, M., Handler, M.R., Baker, J.A., 2010. High-precision Mg isotopic systematics of bulk chondrites. Earth Planet. Sci. Lett. 297 (1–2), 165–173.
Shen, B., Jacobsen, B., Lee, C.-T.A., Yin, Q.-Z., Morton, D.M., 2009. The Mg isotopic systematics of granitoids in continental arcs and implications for the role of chemical weathering in crust formation. Proc. Natl. Acad. Sci. 106 (49), 20652–20657.
Teng, F.-Z., Yang, W., 2014. Comparison of factors affecting the accuracy of high-precision magnesium isotope analysis by multi-collector inductively coupled plasma mass spectrometry. Rapid Commun. Mass Spectrom. 28 (1), 19–24.
Teng, F.-Z., Wadhwa, M., Helz, R.T., 2007. Investigation of magnesium isotope fractionation during basalt differentiation: implications for a chondritic composition of the terrestrial mantle. Earth Planet. Sci. Lett. 261 (1–2), 84–92.
Teng, F.-Z., Li, W.-Y., Ke, S., Marty, B., Dauphas, N., Huang, S., Wu, F.-Y., Pourmand, A., 2010a. Magnesium isotopic composition of the Earth and chondrites. Geochim. Cosmochim. Acta 74 (14), 4150–4166.
Teng, F.-Z., Li, W.-Y., Rudnick, R.L., Gardner, L.R., 2010b. Contrasting lithium and magnesium isotope fractionation during continental weathering. Earth Planet. Sci. Lett. 300 (1–2), 63–71.

Tipper, E.T., Galy, A., Bickle, M.J., 2006. Riverine evidence for a fractionated reservoir of Ca and Mg on the continents: Implications for the oceanic Ca cycle. Earth Planet. Sci. Lett. 247 (3–4), 267–279.
Tipper, E.T., Galy, A., Bickle, M.J., 2008a. Calcium and magnesium isotope systematics in rivers draining the Himalaya-Tibetan-Plateau region: lithological or fractionation control? Geochim. Cosmochim. Acta 72 (4), 1057–1075.
Tipper, E.T., Louvat, P., Capmas, F., Galy, A., Gaillardet, J., 2008b. Accuracy of stable Mg and Ca isotope data obtained by MC-ICP-MS using the standard addition method. Chem. Geol. 257 (1–2), 65–75.
Wang, G., Lin, Y., Liang, X., Liu, Y., Xie, L., Yang, Y., Tu, X., 2011. Separation of magnesium from meteorites and terrestrial silicate rocks for high-precision isotopic analysis using multiple collector-inductively coupled plasma-mass spectrometry. J. Anal. At. Spectrom. 26 (9), 1878–1886.
Wilde, S.A., Valley, J.W., Peck, W.H., Graham, C.M., 2001. Evidence from detrital zircons for the existence of continental crust and oceans on the Earth 4.4[thinsp]Gyr ago. Nature 409 (6817), 175–178.
Wimpenny, J., Colla, C.A., Yin, Q.-Z., Rustad, J.R., Casey, W.H., 2014a. Investigating the behaviour of Mg isotopes during the formation of clay minerals. Geochim. Cosmochim. Acta 128, 178–194.
Wimpenny, J., Yin, Q.-Z., Tollstrup, D., Xie, L.-W., Sun, J., 2014b. Using Mg isotope ratios to trace Cenozoic weathering changes: a case study from the Chinese loess plateau. Chem. Geol. 376, 31–43.
Wombacher, F., Eisenhauer, A., Heuser, A., Weyer, S., 2009. Separation of Mg, Ca and Fe from geological reference materials for stable isotope ratio analyses by MC-ICP-MS and double-spike TIMS. J. Anal. At. Spectrom. 24 (5), 627–636.
Wombacher, F., Eisenhauer, A., Böhm, F., Gussone, N., Regenberg, M., Dullo, W.C., Rüggeberg, A., 2011. Magnesium stable isotope fractionation in marine biogenic calcite and aragonite. Geochim. Cosmochim. Acta 75 (19), 5797–5818.
Xiao, Y., Teng, F.-Z., Zhang, H.-F., Yang, W., 2013. Large magnesium isotope fractionation in peridotite xenoliths from eastern North China craton: product of melt–rock interaction. Geochim. Cosmochim. Acta 115, 241–261.
Yang, W., Teng, F.-Z., Zhang, H.-F., 2009. Chondritic magnesium isotopic composition of the terrestrial mantle: a case study of peridotite xenoliths from the North China craton. Earth Planet. Sci. Lett. 288 (3–4), 475–482.
Young, E.D., Galy, A., 2004. The isotope geochemistry and cosmochemistry of magnesium. Rev. Mineral. Geochem. 55 (1), 197–230.
Young, E.D., Galy, A., Nagahara, H., 2002. Kinetic and equilibrium mass-dependent isotope fractionation laws in nature and their geochemical and cosmochemical significance. Geochim. Cosmochim. Acta 66 (6), 1095–1104.
Young, E.D., Tonui, E., Manning, C.E., Schauble, E., Macris, C.A., 2009. Spinel–olivine magnesium isotope thermometry in the mantle and implications for the Mg isotopic composition of Earth. Earth Planet. Sci. Lett. 288 (3–4), 524–533.